High-Efficiency and Wideband Dual-Resonance Full-Metal Cavity-Backed Slot Antenna Array

Rui-Sen Chen, *Student Member, IEEE*, Lei Zhu, *Fellow, IEEE*, Jing-Yu Lin, *Student Member, IEEE*, Sai-Wai Wong, *Senior Member, IEEE*, Yang Yang, *Senior Member, IEEE*, Yin Li, Long Zhang, *Member, IEEE*, and Yejun He, *Senior Member, IEEE*

***Abstract*—A dual-resonance wideband full-metal cavity-backed slot antenna array (CBSA) with high efficiency is proposed. A cavity mode and a resonant-iris mode are used to produce a wide impedance bandwidth. Radiation slots (elements) placed on the top wall are directly fed by electric fields of the modes using a single feeding slot without extra structures. This simplified feeding structure can reduce the antenna complexity, and can also improve the radiation efficiency by reducing power loss along with the conventional feeding power dividers. Thereafter, two wideband and high-efficiency slot arrays with 2×2 and 4×4 elements are designed based on these two cavity modes and proposed a simplified feeding structure. The measurement of 2×2 slot array shows that the proposed 2×2 slot antenna array can achieve 15% bandwidth, 13.4 dBi peak gain, and 95% total efficiency.**

***Index Terms*—Antenna array, cavity-backed slot antenna (CBSA), dual-resonance, high efficiency, full-metal, simplified feeding structure, wideband.**

I. Introduction

CAVITY-BACKED slot antennas (CBSAs) [1]–[7] have been widely applied to wireless systems requiring high gain and high efficiency for the increasing development of communication technologies. Among them, the full-metal CBSAs [5]–[7] can further improve the gain and efficiency due to the nondielectric loss. Besides, a full-metal structure has a high power capacity. Thus, the full-metal antenna is a good candidate for the long-distance and high-power communication systems, such as satellite and radar communications.

Manuscript received May 1, 2020; revised June 1, 2020; accepted June 5, 2020. Date of publication June 9, 2020; date of current version August 4, 2020. This work was supported in part by the Shenzhen Science and Technology Programs under Grant JCYJ20190808145411289 and Grant JCYJ20180305124543176, in part by the Natural Science Foundation of Guangdong Province under Grant 2018A030313481, and in part by the Shenzhen University Research Startup Project of New Staff under Grant 860-000002110311. *(Corresponding author: Sai-Wai Wong.)*

Rui-Sen Chen is with the College of Electronics and Information Engineering, Shenzhen University, Shenzhen 518060, China, and also with the Department of Electrical and Computer Engineering, Faculty of Science and Technology, University of Macau, Macau 999078, China (e-mail: crs13763378709@163.com).

Lei Zhu is with the Department of Electrical and Computer Engineering, Faculty of Science and Technology, University of Macau, Macau 999078, China (e-mail: leizhu@umac.mo).

Jing-Yu Lin and Yang Yang are with the School of Electrical and Data Engineering, University of Technology Sydney, Ultimo, NSW 2007, Australia (e-mail: l.j.2014@ieee.org; yang.yang.au@ieee.org).

Sai-Wai Wong, Yin Li, Long Zhang, and Yejun He are with the College of Electronics and Information Engineering, Shenzhen University, Shenzhen 518060, China (e-mail: wongsaiwai@ieee.org; liyinuestc@gmail.com; long.zhang@szu.edu.cn; heyejun@126.com).

Digital Object Identifier 10.1109/LAWP.2020.3001057

Due to the high-quality factor and single resonance, conventional CBSAs suffer from narrow bandwidth [1]–[7]. Several approaches have been reported to enhance the bandwidth in open literature. The multimode structure has been utilized to design antennas with enhanced bandwidth [8]–[11]. In [11], a wideband triple-resonance antenna using one cavity mode and two resonant-iris modes is proposed, which can achieve 20% bandwidth. In [12] and [13], a wide slot was used to design wideband slot antennas. In [14] and [15], two filtering slot antennas based on cascade resonant cavities are proposed to overcome the narrowband of slot antenna using a single resonant cavity [1]–[7], the antenna using seven cascade cavities can achieve 10% bandwidth [15]. The corporate-feed technique has been widely used to design wideband waveguide slot array [16]–[21] for the in-phase excitation independent of the frequency. An 8×8 slot antenna array with 36.9% fractional bandwidth is proposed in [21] by using the full-corporate waveguide-fed structure. However, the power dividers utilized in [14]–[21] may increase the complexity and overall size of the slot antenna array.

In this letter, a novel wideband dual-resonance CBSA array in a single cavity with high efficiency is proposed. A cavity mode and a resonant-iris mode are used to form a wide bandwidth. These two modes are explained and analyzed based on the parameter study and their electric field distributions. The radiation slots (elements) placed on the top wall of the cavity are fed directly by the electric fields of the modes without extra power dividers, which can reduce the antenna complexity and also improve the radiation efficiency by eliminating the power loss on the conventional power dividing network. Two wideband antenna arrays with 2×2 and 4×4 slots are then designed. The CST commercial simulator is used to analyze and design the proposed antenna. The measurement shows that the proposed 2×2 slot array can achieve 15% bandwidth, 13.4 dBi peak gain, and >95% total efficiency over the operating bandwidth.

II. Full-Metal Wideband Slot Antenna Array

A. Full-Metal Cavity-Backed 2×2 Slot Antenna Array

Fig. 1 shows the geometry of the 2×2 slot antenna array, which includes a resonant cavity with four radiation slots at the top wall and one feeding slot at the bottom wall, and a coaxial-to-waveguide transition formed by an open-ended feeding cavity and a metal probe. The long sides of the radiation slots and feeding slots are placed in the same direction, i.e., x-axis. Four elements (slots) are fed through a single feeding slot without using extra power dividing network, which can reduce the power loss and enhance the radiation efficiency. Besides, the nonuse of

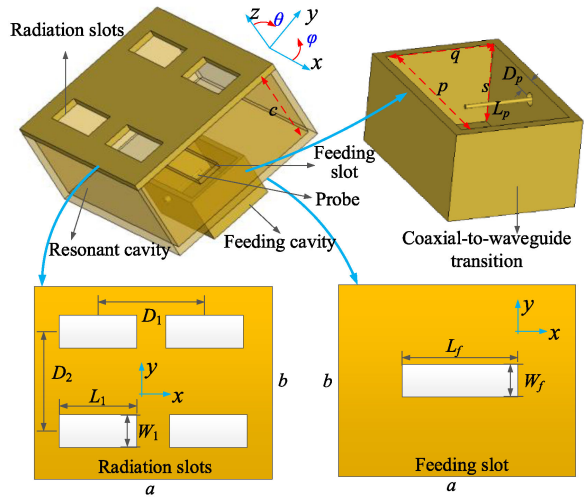

Fig. 1. Geometry of the proposed wideband cavity-backed 2 × 2 slot antenna array. Initial dimensions (Unit: mm): $a = 120$, $b = 100$, $c = 47$, $L_1 = 40$, $W_1 = 15$, $D_1 = 58$, $D_2 = 59$, $p = 52$, $q = 35$, $s = 25$, $L_f = 42$, $W_f = 15$, $L_p = 21$, and $D_p = 6$.

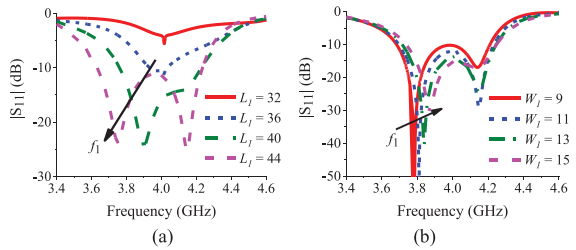

Fig. 2. Adjustment of f_1 and f_2 under the effect of four radiation slots (a) versus length L_1 (for $W_1 = 15$) and (b) versus width W_1 (for $L_1 = 40$).

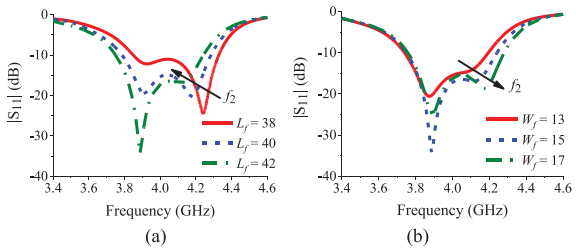

Fig. 3. Adjustment of f_1 and f_2 under the effect of feeding slot (a) versus length L_f (for $W_f = 15$) and (b) versus width W_f (for $L_f = 42$).

power dividers can also obtain a reduced complexity and overall size.

A modified TE_{101} cavity mode and a resonant-iris mode corresponding to the feeding slot [22] are used to form the dual-resonance operating band. To better understand these two modes, some parameter studies are first presented. The resonant frequencies of the proposed two modes are defined as f_1 and f_2, respectively. Fig. 2 indicates that the size of radiation slots only causes the frequency shift of mode f_1. The increasing slot length L_1 and decreasing slot width W_1 cause a decreasing f_1, and the slot length has a larger effect on the frequency shift. Besides, the mode f_1 exists only when L_1 is increased to a relatively large value. In this case, the mode f_1 appears when L_1 is longer than 30 mm, and the reason is that the small slot length cannot produce enough perturbation to generate the mode f_1. Fig. 3 indicates that the varying size of the feeding slot only affect resonant

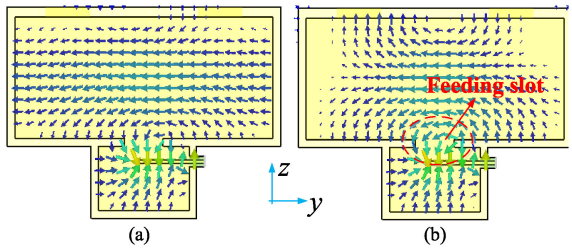

Fig. 4. (a) Electric-field distribution of resonant mode f_1 at 3.88 GHz. (b) Electric-field distribution of resonant mode f_2 at 4.18 GHz.

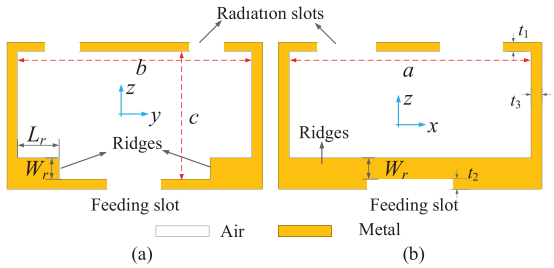

Fig. 5. Modified antenna with loaded ridges. (a) View of the resonant cavity at *yz* plane. (b) View of the resonant cavity at *xz* plane. (Other parts can be referred to Fig. 1.)

frequency f_2, and a larger L_f or a smaller W_f will produce a lower f_2.

The electric field distributions of f_1 and f_2 are provided in Fig. 4(a) and (b), respectively. The obtained frequencies of 3.88 and 4.18 GHz are the two reflection zeros of the simulated $|S_{11}|$ under the initial dimensions provided in Fig. 1. We see that the first mode is a nonstandard cavity mode, which is similar to the TE_{101}, whose resonant frequency is calculated as 3.4 GHz using (1), while the proposed TE_{101}-like mode f_1 resonates at 3.88 GHz. The second mode is a resonant-iris mode, as the electric field mainly distributes around the feeding slot. The calculated frequency of resonant-iris mode using (2) is 4 GHz [11], [22], while the frequency of the proposed resonant-iris mode is 4.18 GHz. According to (2), a larger L_f or a smaller W_f will cause a lower f_{iris}, which matches the tendency of f_2 with varying of L_f and W_f shown in Fig. 3. There is a frequency difference between the calculated ones and simulated ones, while (1) and (2) can explain the effect of the slot length and width on the resonant frequencies and give the guideline to adjust the resonant frequencies.

$$f_{TE_{101}} = \frac{v}{2}\sqrt{\left(\frac{1}{a}\right)^2 + \left(\frac{1}{c}\right)^2} \tag{1}$$

$$f_{\text{iris}} = \frac{v}{2}\sqrt{\frac{b^2 - W_f^2}{b^2 L_f^2 - a^2 W_f^2}} \tag{2}$$

where v represents the light speed in the air, a, b, and c are the side length of the cavity, and L_f and W_f are the length and width of the feeding slot. All the dimensions are marked in Fig. 1.

B. Enhanced Bandwidth With Loaded Ridges

To improve the bandwidth, a modified slot antenna with loaded ridges in the resonant cavity is presented, as shown in Fig. 5. The loaded ridges are placed at the bottom of the cavity, and the long sides of them are along the *x*-axis. The length and

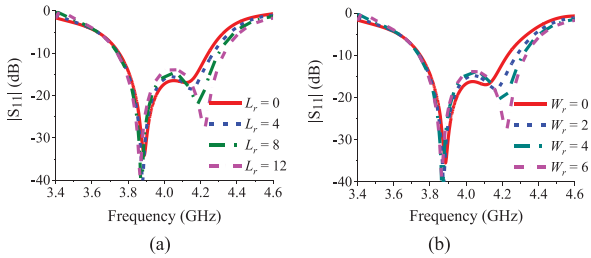

Fig. 6. Adjustment of bandwidth (a) versus L_r (for $W_r = 6$) and (b) versus W_r (for $L_r = 12$).

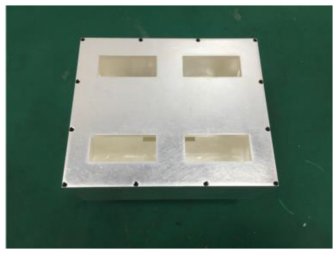

Fig. 7. Photograph of the proposed antenna. Final dimensions (Unit: mm): $a = 120$, $b = 100$, $c = 47$, $L_1 = 40$, $W_1 = 17$, $D_1 = 58$, $D_2 = 59$, $L_f = 42$, $W_f = 15$, $L_r = 12$, $W_r = 6$, $p = 52$, $q = 35$, $s = 25$, $D_p = 6$, $L_p = 21$, $t_1 = 4$, $t_2 = 3$, and $t_3 = 3$.

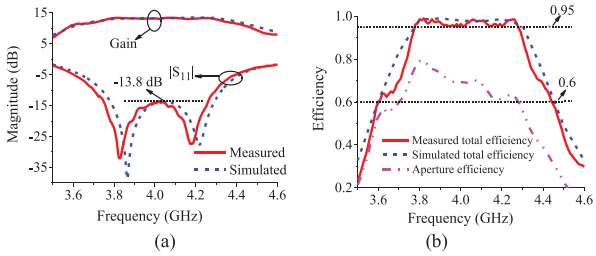

Fig. 8. Measured and simulated results. (a) $|S_{11}|$ and gain. (b) Efficiency.

width of the ridges are expressed as L_r and W_r, respectively. The effect of the loaded ridges is plotted in Fig. 6(a) and (b). It can be seen that the varying L_r and W_r has little effect on f_1, but introduces a frequency shift of f_2. The increasing L_r and W_r produce a decreasing effective b in (2), which then produce a high resonant frequency of f_2. Meanwhile, the increasing L_r and W_r have acceptable deterioration on the impedance matching at the operating frequency, as shown in Fig. 6. Thus, the introduction of the loaded ridges can enhance the bandwidth of the proposed slot antenna array. The bandwidth is increased from 12% to 15% with the effect of the loaded ridges.

III. Antenna Design and Experimental Result

A. 2 × 2 Slot *Antenna* Array

The proposed 2 × 2 slot array slot antenna array is designed and optimized. After the optimization, this antenna is fabricated (using silver-plated brass material) and measured. The photograph of the fabricated antenna is provided in Fig. 7. The measured $|S_{11}|$ and realized gain are shown in Fig. 8(a) with the comparison of simulated results. It can be seen that the measured bandwidth with $|S_{11}| < -10$ dB is about 15% (from 3.69 to 4.31 GHz). The frequency difference between the measured and simulated $|S_{11}|$ is due to the fabrication roughness. The measured in-band (from 3.69 to 4.31 GHz) gain varies from 12.4

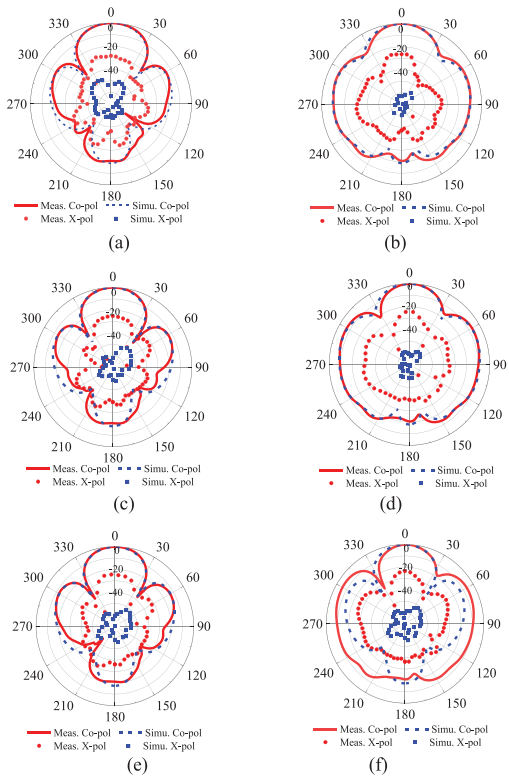

Fig. 9. Measured and simulated radiation patterns. (a) 3.8 GHz at *xz* plane. (b) 3.8 GHz at *yz* plane. (c) 4.1 GHz at *xz* plane. (d) 4.1 GHz at *yz* plane. (e) 4.3 GHz at *xz* plane. (f) 4.3 GHz at *yz* plane.

to 13.4 dBi, and at the band of 3.77–4.29 GHz, the gain varies from 13 to 13.4 dBi. The measured total efficiency is higher than 95% over the operating bandwidth, as shown in Fig. 8(b), which is slightly lower than the simulated total efficiency of 97%. The total efficiency is obtained, including the reflection loss and conductor loss. The high efficiency is obtained due to the full-metal structure and the simplified feeding structure without using power dividers.

The aperture efficiency $\varepsilon_{\rm ap}$ of the antenna is calculated as

$$\varepsilon_{\rm ap} = \frac{G_r \cdot \lambda^2}{4\pi \cdot A} \tag{3}$$

where G_r is the realized gain, λ is the wavelength at the operating frequency, and A is the maximum physical area of the radiation plane. The aperture efficiency of the proposed slot antenna array is plotted in Fig. 8(b) with a dot-dash line, which indicates that the proposed antenna has aperture efficiency higher than 60% over the operating frequency, and the maximum aperture efficiency is about 78% at 3.8 GHz.

Fig. 9 depicts the radiation patterns at 3.8, 4.1, and 4.3 GHz. The measured co-planar polarizations (co-pol) at both *xz* plane and *yz* plane have good agreement with the simulated ones. As the proposed antenna is designed based on two modes with electric field distribution along one direction, as shown in Fig. 4, low cross polarizations (X-pol) can be achieved. The simulated cross polarization is better than −50 dB, as shown in Fig. 9. While the measured cross polarizations are only better than −22 dB, the discrepancy between the measurement and simulation is due to that the tested horn antenna and proposed antenna are not aligned in an ideal angle, i.e., 90°, when testing the cross polarization.

TABLE I
COMPARISONS WITH REPORTED CAVITY SLOT ANTENNA ARRAYS

Ref.	Freq. (GHz)	Elements	FBW	Cavity Type	Power divider	Gain (dBi)	Total Efficiency	Aperture Efficiency	Aperture Size ($\lambda_0 \times \lambda_0$)
[15]	10	4×4	10%#	Full-metal	Yes	20.23~20.43	N.A.	~ 70%	N.A.
[17]	61.5	16×16	8.3%$	Full-metal	Yes	> 32 Peak: 33	83.6%	~ 59%	15.4×15.6
[19]	15.2	16×16	13.8%*	Full-metal	Yes	> 29.5	N.A.	> 70%	12.16×12.16
[20]	13.6	16×16	17.1%*	Full-metal	Yes	29.5~31.4	N.A.	> 70% Peak: 85%	10.88×10.88
[21]	12.5	8×8	36.9%*	Full-metal	Yes	23.4~26.3	> 90%	> 60%	6.71×6.71
This work (2×2)	4	2×2	15%#	Full-metal	No	12.4~13.4	> 95%	> 60% Peak: 78%	1.68×1.41
This work (4×4) Simulated	4.08	4×4	12%#	Full-metal	No	15.7~18.4	> 95%	> 50% Peak: 68%	2.98×2.65

FBW: Fabrication bandwidth; N.A.: Not available.
#FBW with $|S_{11}| < -10$ dB.
*FBW with VSWR < 2 ($|S_{11}| < -9.5$ dB).
$FBW with VSWR < 1.5 ($|S_{11}| < -14$ dB).

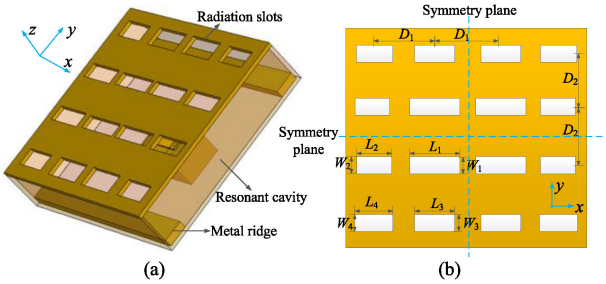

Fig. 10. Proposed wideband 4 × 4 slot array. (a) Full view. (b) Top view. Final dimensions (Unit: mm): $a = 220$, $b = 195$, $c = 43$, $L_1 = 51$, $W_1 = 16$, $L_2 = 35$, $W_2 = 18$, $L_3 = 42$, $W_3 = 18$, $L_4 = 36$, $W_4 = 14$, $D_1 = 55$, $D_2 = 52$, $L_f = 36$, $W_f = 8$, $L_r = 22$, $W_r = 10$, $p = 60$, $q = 35$, $s = 25$, $D_p = 4$, $L_p = 21$, $t_1 = 8$, $t_2 = 2$, and $t_3 = 3$.

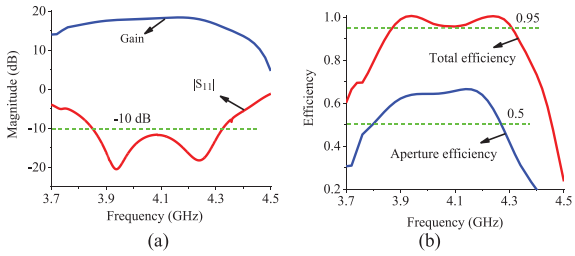

Fig. 11. Simulated results. (a) $|S_{11}|$ and gain. (b) Efficiency.

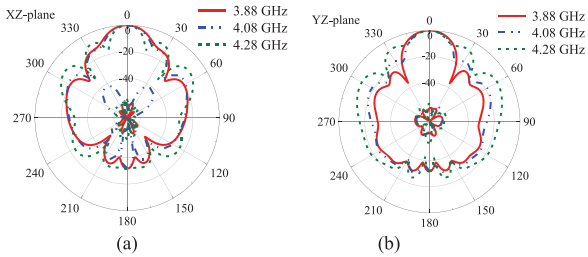

Fig. 12. Simulated radiation patterns at 3.88, 4.08, and 4.38 GHz. (a) *xz* plane. (b) *yz* plane.

B. 4 × 4 Slot Antenna Array

To further show the feasibility of the proposed design concept, a wideband 4 × 4 slot array in a single resonant cavity is presented, as shown in Fig. 10. The marked dimensions of the slot size and distance between slots are provided in the figure, while other dimensions can be referred to Figs. 1 and 5. The radiation slots are symmetrically arranged along the *x*-axis and *y*-axis. The two modes shown in Fig. 4 are retained to obtain a wide bandwidth. Similar to the 2 × 2 slot array, all the radiation slots are fed by the electric field of the two modes without using extra power dividers. The purpose of nonidentical radiation slots is to optimize the performance of the antenna, such as the impedance matching and radiation gain.

After the optimization, the simulated results are provided in Figs. 11 and 12. From Fig. 11, we see that the antenna can achieve 12% bandwidth from 3.84 to 4.33 GHz with $|S_{11}| < -10$ dB, and the in-band radiation gain varies from 15.7 to 18.4 dBi. In the band of 3.85 to 4.25 GHz, this antenna has gain >17 dBi, total efficiency >95% (including reflection loss and conductor loss), and aperture efficiency > 50% (peak: 68%). The radiation patterns are shown in Fig. 12, which indicates that this antenna has cross polarization better than −40 dB.

The comparison with other reported wideband slot antennas is provided in Table I. It can be seen that the proposed slot antenna array has a wide bandwidth, high efficiency, and low design complexity, especially no power divider is required. Although the works presented in [20] and [21] have wider fractional bandwidth, they require a large and complicated 3-D division network and each division session also works as a wideband impedance matching circuit.

IV. CONCLUSION

A wideband full-metal CBSA array with high efficiency is proposed in this letter. A dual-resonance cavity resonator with a cavity mode and a resonant-iris mode is used to design the wideband slot antenna. The nonuse of power dividers for feeding the array elements introduces the high efficiency and reduces the antenna complexity. Two slot array with 2 × 2 and 4 × 4 elements are presented to show the feasibility of the proposed design concept. The final measurement shows that the proposed 2 × 2 antenna array can achieve 15% bandwidth, 13.4 dBi peak gain, and 95% total efficiency.

REFERENCES

[1] G. Q. Luo, Z. F. Hu, L. X. Dong, and L. L. Sun, "Planar slot antenna backed by substrate integrated waveguide cavity," *IEEE Antennas Wireless Propag. Lett.*, vol. 7, pp. 236–239, 2008.

[2] L. Ge, Y. Li, J. Wang, and C.-Y.-D. Sim, "A low profile reconfigurable cavity-backed slot antenna with frequency, polarization, and radiation pattern agility," *IEEE Trans. Antennas Propag.*, vol. 65, no. 5, pp. 2182–2189, May 2017.

[3] R. Bayderkhani, K. Forooraghi, and B. Abbasi-Arand, "Gain-enhanced SIW cavity-backed slot antenna with arbitrary levels of inclined polarization," *IEEE Antennas Wireless Propag. Lett.*, vol. 14, pp. 931–934, 2015.

[4] W. Li, K. D. Xu, X. Tang, Y. Yang, Y. Liu, and Q. H. Liu, "Substrate integrated waveguide cavity-backed slot array antenna using high-order radiation modes for dual-band applications in *K*-Band," *IEEE Trans. Antennas Propag.*, vol. 65, no. 9, pp. 4556–4565, Sep. 2017.

[5] D. D. de Schweinitz and C. S. Lee, "Rectangular cavity-backed 4-slot antenna," *IEEE Trans. Antennas Propag.*, vol. 49, no. 12, pp. 1718–1722, Dec. 2001.

[6] J.-Y. Lin *et al.*, "A dual-functional triple-mode cavity resonator with the integration of filters and antennas," *IEEE Trans. Antennas Propag.*, vol. 66, no. 5, pp. 2589–2593, May 2018.

[7] Y.-M. Wu, S.-W. Wong, J.-Y. Lin, L. Zhu, Y. He, and F.-C. Chen, "A circularly-polarized cavity-backed slot antenna with enhanced radiation gain," *IEEE Antennas Wireless Propag. Lett.*, vol. 17, no. 6, pp. 1010–1014, Jun. 2018.

[8] G. Q. Luo, Z. F. Hu, W. J. Li, X. H. Zhang, L. L. Sun, and J. F. Zheng, "Bandwidth-enhanced low-profile cavity-backed slot antenna by using hybrid SIW cavity modes," *IEEE Trans. Antennas Propag.*, vol. 60, no. 4, pp. 1698–1704, Apr. 2012.

[9] S. Mukherjee, A. Biswas, and K. V. Srivastava, "Broadband substrate integrated waveguide cavity-backed bow-tie slot antenna," *IEEE Antennas Wireless Propag. Lett.*, vol. 13, pp. 1152–1155, 2014.

[10] Y. Shi, J. Liu, and Y. Long, "Wideband triple- and quad-resonance substrate integrated waveguide cavity-backed slot antennas with shorting vias," *IEEE Trans. Antennas Propag.*, vol. 65, no. 11, pp. 5768–5775, Nov. 2017.

[11] Y.-M. Wu, S.-W. Wong, H. Wong, and F.-C. Chen, "A design of bandwidth-enhanced cavity-backed slot filtenna using resonance windows," *IEEE Trans. Antennas Propag.*, vol. 67, no. 3, pp. 1926–1930, Mar. 2019.

[12] J. Hirokawa, H. Arai, and N. Goto, "Cavity-backed wide slot antenna," *Proc. Inst. Elect. Eng.*, vol. 136, no. 1, pp. 29–33, Feb. 1989.

[13] K. Gong, Z. N. Chen, X. M. Qing, P. Chen, and W. Hong, "Substrate integrated waveguide cavity-backed wide slot antenna for 60 GHz bands," *IEEE Trans. Antennas Propag.*, vol. 60, no. 12, pp. 6023–6026, Dec. 2012.

[14] F.-C. Chen, J.-F. Chen, Q.-X. Chu, and M. J. Lancaster, "X-band waveguide filtering antenna array with nonuniform feed structure," *IEEE Trans. Microw. Theory Techn.*, vol. 65, no. 12, pp. 4843–4850, Dec. 2017.

[15] R. H. Mahmud and M. J. Lancaster, "High-gain and wide-bandwidth filtering planar antenna array-based solely on resonators," *IEEE Trans. Antennas Propag.*, vol. 65, no. 5, pp. 2367–2375, May 2017.

[16] B. Lee, K. Jung, and S. Yang, "High-efficiency planar slot array antenna with a single waveguide-fed cavity-backed subarray," *Microw. Opt. Technol. Lett.*, vol. 43, no. 3, pp. 228–231, Nov. 2004.

[17] Y. Miura, J. Hirokawa, M. Ando, Y. Shibuya, and G. Yoshida, "Double-layer full-corporate-feed hollow-waveguide slot array antenna in the 60 GHz band," *IEEE Trans. Antennas Propag.*, vol. 59, no. 8, pp. 2844–2851, Aug. 2011.

[18] T. Tomura, J. Hirokawa, T. Hirano, and M. Ando, "A 45 linearly polarized hollow-waveguide 16×16-slot array antenna covering 71-86 GHz band," *IEEE Trans. Antennas Propag.*, vol. 62, no. 10, pp. 5061–5067, Oct. 2014.

[19] G. L. Huang, S. G. Zhou, T. H. Chio, H. T. Hui, and T. S. Yeo, "A low profile and low sidelobe wideband slot antenna array feb by an amplitude-tapering waveguide feed-network," *IEEE Trans. Antennas Propag.*, vol. 63, no. 1, pp. 419–423, Jan. 2015.

[20] S.-G. Zhou, G.-L. Huang, T.-H. Chio, J.-J. Yang, and G. Wei, "Design of a wideband dual-polarization full-corporate waveguide feed antenna array," *IEEE Trans. Antennas Propag.*, vol. 63, no. 11, pp. 4775–4782, Nov. 2015.

[21] S.-G. Zhou, G.-L. Huang, Z.-H. Peng, and L.-J. Ying, "A wideband full-corporate-feed waveguide slot planar array," *IEEE Trans. Antennas Propag.*, vol. 64, no. 5, pp. 1974–1978, May 2016.

[22] T.-S. Chen, "Characteristics of waveguide resonant-iris filters," *IEEE Trans. Microw. Theory Techn.*, vol. MTT-15, no. 4, pp. 260–262, Apr. 1967.